4-15-2020

Approximate Solutions to the Allen-Cahn Equation Using the Finite Difference Method

Jamil Malik Villarreal

APPROXIMATE SOLUTIONS TO THE ALLEN-CAHN EQUATION USING THE FINITE DIFFERENCE METHOD

A Thesis

by

JAMIL MALIK VILLARREAL

Submitted to Texas A&M International University
in partial fulfillment of the requirements
for the degree of

MASTER OF SCIENCE

MAY 2016

Major Subject: Mathematics

APPROXIMATE SOLUTIONS TO THE ALLEN-CAHN EQUATION USING THE FINITE DIFFERENCE METHOD

A Thesis

by

JAMIL MALIK VILLARREAL

Submitted to Texas A&M International University
in partial fulfillment of the requirements
for the degree of

MASTER OF SCIENCE

Approved as to style and content by:

Chair of Committee,	Runchang Lin
Committee Members,	David K. Milovich
	Rohitha H. Goonatilake
	Juan H. Hinojosa
Head of Department,	Rohitha H. Goonatilake

MAY 2016

Major Subject: Mathematics

ABSTRACT

Approximate Solutions to the Allen-Cahn Equation Using the Finite Difference Method (May 2016)

Jamil Malik Villarreal, B.S., Texas A & M International University, May 2014;

Chair of Committee: Dr. Runchang Lin

Seeking a deeper understanding of the world has been a driving factor in Applied Mathematics. From counting and measuring physical objects to developing equations and ratios that resemble patterns in nature, mathematics is used to interpret and explain the intricate structures that we observe everyday. The field of Applied Mathematics almost always involves setting up and then solving, or approximating solutions to, at least one partial differential equation that takes the physical and mathematical properties into consideration. This is the process of creating mathematical models.

For this thesis, we will investigate approximate solutions to the Allen-Cahn equation whose analytic solution is still unknown due to the nonlinearities of the problem as well as its sensitivity to certain constants as we shall see. The numerical schemes involved in these approximations are obtained from the finite difference method.

ACKNOWLEDGMENTS

I would like to first of all thank God for my life. I would also like to thank my family for always supporting me and encouraging me to always strive for the best. When times get rough, they always remind me of the importance of being diligent and humble. Regardless of any outcome, we will always have each other and that is what truly matters. I would like to thank all of my friends who showed me how to have a good time and celebrate all the small accomplishments that eventually add up to this remarkable achievement.

This research is partially supported by NSF DMS 1217268 and a TAMIU University Research Development Award.

TABLE OF CONTENTS

Page

LIST OF TABLES

Page

LIST OF FIGURES

Page

CHAPTER I

BACKGROUND INFORMATION

About 36 years ago in 1979, John W. Cahn and his graduate student Sam M. Allen studied how materials involving iron alloys interact with each other. Seeking to describe the motion of anti-phase boundaries in binary metallic alloys led them to create a phase-field model that allows for topological changes. Anti-phase boundaries can be thought of as the boundary between one wave and another at a particular point in time. Their motivating factor was to create a complete, coherent theory of interfacial motion in solids that takes the geometry of the interface, excess free energy, and the topological nature of interfaces into consideration in order to have a more definite picture of these microstructures [2]. From a mathematical point of view, the popular relationship between interfacial velocity V and thermodynamic driving forces (i.e. decrease in free energy) was investigated: $V = \mu\sigma(K_1 + K_2)$, where μ is the mobility, $(K_1 + K_2)$ is the mean of local principal curvatures of the boundary of the domain, and σ is the excess free energy per unit area. We can interpret the interfacial velocity V as the velocity of the front across which the phases are different; that is to say, it is like tracking a boundary between the two domains of consideration.

By using iron-aluminum alloys and applying heat to simulate the interaction of materials thereby creating anti-phase boundaries, the experimental data shows that interface velocity is not necessarily proportional to thermodynamic driving forces. Hence their original hypothesis needed some modification. Nonetheless, their theory does highlight three important factors to consider when it comes to antiphase boundaries: this approach is only legitimate for phases with order-disorder reaction rates that are higher than first-order, the energy in an antiphase boundary must be isotropic (i.e., constant value regardless of the direction of measurement), and the possibility of more than one antiphase boundary within the domain of consideration. Although their work stopped here, the disproportionality of thermodynamic driving forces to interfacial velocity spawned a very active research field in partial differential equations as well as the numerical analysis behind their approximate solutions.

The journal model used is from the *International Journal of Computer Mathematics.*

CHAPTER II

LITERATURE REVIEW

There has been considerable investigations done on the Allen-Cahn equation that ranges from numerical experiments to analytical behavior around singularities (points where a function is not defined) in order to establish some error bounds and asymptotic limits. Hence, there is a very large pool of references that deal with the equation we are interested in. Based on the goals explained in Chapter 3, we have consulted specific works that share our numerical interests. A brief annotated bibliography is provided below.

In [2], the pioneering work of Sam Allen and his professor John W. Cahn was first introduced and is referred to as the Allen-Cahn equation later. They focus on curved antiphase boundaries (APB) by treating them as surfaces with geometrical properties such as area and curvature, thermodynamic and chemical properties such as excess free energy per unit area and adsorption, and kinetic properties such as their velocity in response to a driving force. A thorough treatment of interface motion and anti-phase boundary motion is sought.

From [11], cylindrically symmetric traveling wave solutions to the Allen-Cahn equation has been investigated. The author seeks results that use interfaces which travel upwards in the vertical z direction at a uniform speed denoted by c. The Allen-Cahn equation is reformulated for $u = u(x, z, t)$ as

$$u_t = u_{zz} + \Delta u - f(u), \quad x \in \mathbb{R}^n, \quad z \in \mathbb{R}, \quad t > 0.$$

The term appearing on the right-hand side of the equation above is known as the Laplacian, and is defined as the sum of the second-order derivatives of two variables: $\Delta = \frac{\partial^2 u}{\partial x^2} + \frac{\partial^2 u}{\partial y^2}$. Also, the function $f(u)$ is considered to be a nonlinear reaction term. Supposing that a solution to the above development has the form $u(x, z, t) = U(x, z - ct)$, then (c, U) is labeled as a traveling wave solution with profile U and speed c. Furthermore, solutions of the type (c, U) meet the following conditions:

$$\begin{cases} cU_z + U_{zz} + \Delta U = f(U), & \forall x \in \mathbb{R}^n, z \in \mathbb{R}, \\ \lim\limits_{z \to \pm\infty} U(x, z) = \pm 1, & \forall x \in \mathbb{R}^n. \end{cases}$$

Two theorems are proved which show the existence of cylindrically symmetric solutions under certain conditions and asymptotic limits are derived for the level sets of such solutions. On the last page, a heuristic interpretation of the level sets is given for at least two dimensions and the role of curvature for the behavior of the interface is confirmed.

The analytical approach in [1] sheds light on the motion and generation of interfaces. Their main result is that a solution of an Allen-Cahn type equation

$$u_t = \Delta u + \epsilon^{-2} f^{\epsilon}(x, t, u),$$

where $0 < \epsilon < 1$ and $f^{\epsilon}(x, t, u) = f(u) - \epsilon g^{\epsilon}(x, t, u)$ is a bistable nonlinearity associated with a double-well potential, develops a steep transition layer within the time scale of order $\epsilon^2 |ln(\epsilon)|$ that obeys a law of motion whose formal asymptotic limit has an error margin of order ϵ. In regards to our investigation, we let $g \equiv 0$ in the above function definition so that we only have $f(u)$ as the reaction term.

In the seminal work of [3], a very flexible error analysis is conducted based on several numerical simulations of Allen-Cahn type equations. In particular, the authors focus on the following phase-field model version of the Allen-Cahn equation:

$$\begin{aligned} \partial_t u - \Delta u + \epsilon^{-2} f(u) = 0 \quad &\text{in } (0, T) \times \Omega, \\ \partial_n u = 0 \quad &\text{on } (0, T) \times \partial\Omega, \\ u(0, \cdot) = u_0, & \end{aligned}$$

where $T > 0$, $\Omega \subset \mathbb{R}^d, d = 2, 3$, $f(u) = u^3 - u$, and $0 < \epsilon \ll 1$. Recent investigations referenced in this paper have obtained optimal a priori error estimates for the finite element approximation of the above equation which bypass using the maximum principle and have dependence on ϵ^{-1} up to a low order polynomial. This was achieved by using uniform bounds for the principal eigenvalue of the linearized Allen-Cahn operator around the solution $u(t, \cdot)$:

$$-\lambda_{AC}(t) := \inf_{v \in H^1(\Omega) \setminus \{0\}} \frac{||\Delta v||^2_{L^2(\Omega)} + \epsilon^{-2}(f'(u(t))v, v)}{||v||^2_{L^2(\Omega)}}$$

with $(\cdot,\cdot)$ being the inner product in $L^2(\Omega)$. For clarity, $L^2(\Omega)$ refers to the set of square-integrable functions, the input Ω stands for the domain of consideration where the integration is to be carried out, and $H^1(\Omega)$ is a first-order Sobolev space which is defined below. Also, the derivatives of functions in the space $L^2(\Omega)$ can be defined without using a difference quotient, yet they still retain their continuity and classical meaning. With a clever use of integration by parts, we can define a weak derivative, following in the steps of [7], as follows: let $f \in L^2(a,b)$. A function $g \in L^2(a,b)$ is called a *weak derivative* of f if

$$\int_a^b g(s)\psi(s)ds = -\int_a^b f(s)\psi'(s)ds$$

for all $\psi \in C_1^0[a,b]$. The space that contains all weakly differentiable functions, $H^1(a,b) := \{f \in L^2(a,b) | f \text{ has a weak derivative}\}$ is called the first order Sobolev space.

Based on these results, approximations of a large class of evolutions that develop singularities are robustly controlled by revising the approach that established the optimal errors. The proposed bound

$$\int_0^T \lambda_{AC}^+(t)dt \leq C_0 + \log(\epsilon^{-\kappa}),$$

where $x^+ := \max(x,0)$ is a uniform bound up to ϵ^{-1} and the logarithm models transition regions where λ_{AC} decays from ϵ^{-2} to a value that is not related to ϵ. Also, a uniform bound $\lambda_{AC}(t) \leq C$ for almost every $t \in (0,T)$ eliminates generic singularities, or in other words, it accounts for topological changes of the interface. Numerical experiments provided in this publication verify that the proposed bound is feasible, thus leading to its robust a priori error analysis.

A more analytic interpretation of the Allen-Cahn type equations can be found in [14]. In this Ph.D. dissertation, Fang Zhang considers entire solutions of the Allen-Cahn equation that uses a double-well potential that can be either balanced or unbalanced. The term "entire solution" used here refers to solutions that are defined entirely in time and in Euclidean space as opposed to just being specified in the latter. Furthermore, the author classifies every entire solution that satisfies the property of being bistable, or connecting the two-stable states of the Allen-Cahn equation in one spatial variable.

Discrete approximations to the Allen-Cahn equation are addressed in [15]. Moreover, their

approach involves the convergence of numerical approximations of the Allen-Cahn equation in the sharp interface limit. The term "sharp interface" is a very common adjective used not only in this work, but in several other titles as well. Starting by introducing a scaling parameter ϵ that regulates spacial units by ϵ and time-scales by ϵ^2, the following form of the Allen-Cahn equation is studied:

$$\phi_t = \Delta\phi + \frac{1}{\epsilon^2}\phi\left(\phi^2 - 1\right).$$

Here, ϕ is known as the phase field function or order parameter and the width of the diffuse interface is calibrated by ϵ which is strictly positive. Seeking a numerical estimate, the variational interpretation of the Allen-Cahn equation is used to resemble the gradient flow of the energy

$$\mathcal{E}(\phi) = \int_\Omega \left\{ \frac{1}{2}|\nabla\phi|^2 + \frac{1}{4\epsilon^2}(\phi^2 - 1)^2 \right\} d\Omega.$$

The behavior of the solutions to the Allen-Cahn equation, as ϵ goes to zero, are expected to operate like a piecewise constant function with values of ± 1 within the two regions that are separated by a diffusive interfacial layer with thickness of $O(\epsilon)$. This limiting behavior is precisely what is referred to as the sharp interface limit.

In regards to the approach considered in this thesis, the development of a modified finite-difference scheme from [12] motivates us to apply it to the Allen-Cahn equation. While their method is applied to the Fitz-Hugh Nagumo equations in one dimension, our goal is to use this technique on the two dimensional reaction-diffusion equation of Allen-Cahn and examine the results. We describe our results in Chapter 4 as well as provide an analysis for the choice of time and spatial steps in our finite mesh.

CHAPTER III

REACTION-DIFFUSION EQUATIONS AND NUMERICAL METHODS

For completeness, we include a brief review of two popular numerical methods used in solving/approximating partial differential equations as well as a background on the type of equation we are working with.

Generally speaking, this class of PDE's arises in mathematical modeling, typically, when the reactions and disbursements (diffusion) of either one or several materials are considered. By first examining the one-dimensional case, let $u(x,t)$ be a function representing the concentration of a certain chemical at time t with position x on the real line. Our reaction-diffusion equation will then look like

$$\frac{\partial u}{\partial t} = D_u \frac{\partial^2 u}{\partial x^2} + f(u).$$

Here, the function $f(u)$ is the reaction term and is often nonlinear due to the physical background of the problem. It describes the growth or decay of u based on its local behavior. The coefficient D_u is called the diffusive term and models how u "spreads out" within the domain of consideration. Additionally, the word diffusion is derived from the Latin word *diffundere* which means to pour out. It was not until the 1800s when physicists used diffusion to depict how the particles in solids, liquids, and gases interacted and migrate from areas of high concentration to areas of low concentration without joining together. Moreover, it was the German physician Adolf Fick who came to this conclusion by mathematically describing diffusion as

$$\frac{\partial c}{\partial t} = D \frac{\partial^2 c}{\partial x^2}$$

which led to its epithet of Fick's Second Law.

In the following derivation, we will adhere very closely to the macroscopic approach chronicled in [8], although it should be mentioned that there are other techniques that can be used to deduce Fick's Second Law. More rigorous details can be found in [8] and the references therein. Let $c(x,t)$ be the concentration of a chemical and $q(x,t)$ be the flux of $c(x,t)$. Also, we make use of Fick's First Law of Diffusion: $q = -D\nabla c$ where $D(x,t)$ is a diffusion coefficient not depending

on c. This is the mathematical explanation of how materials move from areas of high concentration to areas of low concentration. Furthermore, we also rely on conservation of mass on a constantly closed volume V with a boundary surface of ∂V to describe how the change in total concentration is equal to the change of concentration inside the volume subtracted from the instantaneous efflux of the chemical from V. Mathematically speaking, this is written as

$$\frac{d}{dt}\int_V cdV = -\int_{\partial V} q \cdot ndS$$

and after a clever substitution and application of the divergence theorem, we arrive to

$$\frac{d}{dt}\int_V cdV = \int_V \nabla \cdot (D\nabla c)dV,$$

which will finally show that

$$\int_V \left[\frac{\partial c}{\partial dt} - \nabla \cdot (D\nabla c)\right] dV = 0.$$

Because we are considering a general volume V, the integrand above is exactly zero, hence, $\frac{\partial c}{\partial t} = \nabla \cdot (D\nabla c)$. This equation should look familiar to those who have studied partial differential equations before - it is the famous heat equation if we combine the two gradient operators as ∇^2 which is also known to be the Laplacian operator : $\Delta u = \nabla^2 u = \frac{\partial^2 u}{\partial x^2} + \frac{\partial^2 u}{\partial y^2}$. Since our goal is to find a numerical approximation of a certain type of reaction-diffusion equation, we would need to discuss some of the popular techniques in discretizing continuous operations such as a derivative and the Laplacian. On top of that, we also need to reformulate the continuous domain using a discrete mesh with uniform spacing between elements in either direction. Namely, we will focus on the Finite Difference Method due to its direct implementation in MATLAB.

The main idea behind the Finite Difference Method is that the continuous derivative(s) is/are approximated through linear combinations of function values at certain mesh points. The error between the numerical solution and the exact solution, if it is known, can be determined by the difference between the two at specified points. As we shall see shortly, this error is inherited by the fact that our approximate solution uses a finite part of a Taylor series. Algebraically speaking, this is what a derivative looks like:

$$\begin{aligned}\frac{\partial u}{\partial x}(x) &= \lim_{h\to 0}\frac{f(x+h)-f(x)}{h}\\ &= \lim_{h\to 0}\frac{f(x)-f(x-h)}{h}\\ &= \lim_{h\to 0}\frac{f(x+h)-f(x-h)}{2h}.\end{aligned}$$

Based on this definition, we consider a forward, backwards, and central difference scheme. For simplicity, let us consider the one-dimensional interval $\Omega = (0, X)$ with grid points, also called nodes, $x_i = ihx$ for $i = 0, 1, \ldots, N$, a mesh-function $u_i \approx u(x_i)$, and a mesh with step size $\frac{X}{N}$. Then the forward, backwards, and central difference schemes may be written as

$$\left.\frac{\partial u}{\partial x}\right|_i = \frac{u_{i+1}-u_i}{h} + O(h),$$

$$\left.\frac{\partial u}{\partial x}\right|_i = \frac{u_{i-1}-u_i}{h} + O(h),$$

$$\left.\frac{\partial u}{\partial x}\right|_i = \frac{u_{i+1}-u_{i-1}}{2h} + O(h^2),$$

respectively. Next, the use of Taylor series expansions around a node x_i allows us to write $u(x) = \sum_{n=0}^{\infty}\frac{(x-x_i)^n}{n!}\left(\frac{\partial^n u}{\partial x^n}\right)\Big|_i$ for any function $u \in C^\infty([0, X])$. The space $C^\infty([0, X])$ contains all continuously differentiable functions in the interval $[0, X]$.

Look at the truncation errors:

$$T_1 = u_{i+1} = u_i + h\left(\frac{\partial u}{\partial x}\right)_i + \frac{h^2}{2}\left(\frac{\partial^2 u}{\partial x^2}\right)_i + \frac{h^3}{6}\left(\frac{\partial^3 u}{\partial x^3}\right)_i + \ldots$$

$$T_2 = u_{i-1} = u_i - h\left(\frac{\partial u}{\partial x}\right)_i + \frac{h^2}{2}\left(\frac{\partial^2 u}{\partial x^2}\right)_i - \frac{h^3}{6}\left(\frac{\partial^3 u}{\partial x^3}\right)_i + \ldots$$

Hence, we can derive the forward, backwards, and central difference approximations. Below we provide only the first and second-order partial derivatives, but the process is easily gener-

alized to higher dimensions.

$$T_1 \Rightarrow \left(\frac{\partial u}{\partial x}\right)_i = \frac{u_{i+1} - u_i}{h} - \dots$$

Forward Difference Scheme. Truncation order $O(h)$.

$$T_2 \Rightarrow \left(\frac{\partial u}{\partial x}\right)_i = \frac{u_i - u_{i-1}}{h} + \dots$$

Backward Difference Scheme. Truncation order $O(h)$.

$$T_1 - T_2 \Rightarrow \left(\frac{\partial u}{\partial x}\right)_i = \frac{u_{i+1} - u_{i-1}}{2h} + \dots$$

Central Difference Scheme. Truncation order $O(h^2)$.

$$T_1 + T_2 \Rightarrow \left(\frac{\partial^2 u}{\partial x^2}\right)_i = \frac{u_{i+1} - 2u_i + u_{i-1}}{h^2} + \dots$$

Central Difference Second-Order Scheme. Truncation order $O(h^2)$.

Based on these formulas, we can create a numerical scheme where every continuous operation is replaced with its discrete counterpart. A standardized second-order approach that we will consider first is that of Crank-Nicolson [6] where the spatial derivatives are approximated with the central-difference and the average between the current and the next time step is used. This approach is a combination of the forward difference for the current time level and the backward difference for the following time step. After introducing the Allen-Cahn equation below, the results of this popular numerical scheme are reported in Chapter 4. Furthermore, we also apply a special finite difference scheme developed in [12], but with the Allen-Cahn equation as opposed to the Fitz-Hugh Nagumo equations as originally proposed. These results are included in the fourth chapter of this thesis.

The numerical scheme below was used to solve the Allen-Cahn equation by implementing the Crank-Nicolson method on a uniformly-spaced square grid with zero boundary conditions:

$$\left[2+4r-(U_{i,j}^{n+1}+1)(U_{i,j}^{n+1}-1)\right]U_{i,j}^{n+1}-r\left[U_{i+1,j}^{n+1}+U_{i-1,j}^{n+1}+U_{i,j+1}^{n+1}+U_{i,j-1}^{n+1}\right]$$

$$=$$

$$\left[2-4r+(U_{i,j}^{n}+1)(U_{i,j}^{n}-1)\right]U_{i,j}^{n}+r\left[U_{i+1,j}^{n}+U_{i-1,j}^{n}+U_{i,j+1}^{n}+U_{i,j-1},\right]$$

where we let $r=\frac{\tau}{h^2}$. Notice that the two rates of change involved in the mathematical model are collected using a ratio; specifically, the rate of change in time should have a relation to the rate of change in space if we seek to find reasonable numerical solutions to partial differential equations. This classical numerical scheme has a convergence rate of $O(\tau^2+h^2)$. Our main interest was to use the modified finite difference method that is outlined in [12] to the Allen-Cahn equation with a circular domain for our investigation. That is to say, we can expect to capture a rounded diffusive pattern similar to the one we saw when the Crank-Nicolson method was implemented. For the time dimension, a linear combination of a first and second-order estimate is used whereas the two spatial dimensions are approximated using a second-order central difference. As such, we also report this scheme below

$$(2-\alpha)U_{i,j}^{n+1}-r\left(U_{i+1,j}^{n+1}+U_{i-1,j}^{n+1}+U_{i,j+1}^{n+1}+U_{i,j-1}^{n+1}-4U_{i,j}^{n+1}\right)-\tfrac{2\tau}{\epsilon^2}U_{i,j}^{n+1}f(U_{i,j}^{n})$$

$$=$$

$$2(1-\alpha)U_{i,j}^{n}+r\left(U_{i+1,j}^{n}+U_{i-1,j}^{n}+U_{i,j+1}^{n}+U_{i,j-1}^{n}-4U_{i,j}^{n}\right)+\alpha U_{i,j}^{n-1}$$

where $\alpha\in(0,1)$. Similar to our Crank-Nicolson scheme, we let $r=\frac{\tau}{h^2}$ be the ratio of the two rates of change, but notice that the last term on the left-hand side involves a product of two approximate solutions at separate time-levels. In order to be consistent with our original nonlinear reaction term, we let $f(U_{i,j}^{n})={U_{i,j}^{n}}^2-1$. An illustration of this numerical solution is shown in Figure **??**.

1. Stability Analysis

A very well-known and widely used technique to determine how accurate a numerical scheme is while successively taking the computational errors from the previous step into account

is the Von Neumann stability analysis. The main concern behind this procedure is to have some estimate on how to control the truncation errors at each step of a finite-difference scheme. In order to achieve this, we consider a Fourier expansion in space of our function and compare the proportions of consecutive terms. However when applying this to a finite-difference scheme, one usually collects the discrete rates of change as a ratio so that we can determine how they should be chosen in order to avoid magnifying approximation errors. Let $u(x, y, t)$ be a solution to the Allen-Cahn equation and let $U_{i,j}^n$ be the numerical approximation to u at time level n with location i, j in a finite mesh. Then the Von Neumann stability analysis is done by assuming we have a Fourier expansion of our function

$$u(x, y, t) = \sum_{k=1}^{\infty} c_k e^{I(xi+yj)\theta},$$

where we let I be the complex number $\sqrt{-1}$, and then establishing the following inequality:

$$|\frac{c_{k+1}}{c_k}| \leq 1.$$

For the approach taken in this thesis, we use the modified finite difference method in [12] to the Allen-Cahn equation and seek to find sufficient bounds on the proportion of step sizes related to time and space in our numerical scheme. Moreover, we use the Von Neumann stability analysis outlined above to find a way to control the way we choose our time and spatial steps for our approximate solutions to the Allen-Cahn equation. The following nomenclature is used to simplify the appearance of our numerical scheme

$$k_1 U_{i-1,j}^{n+1} + k_2 U_{i+1,j}^{n+1} + k_1 U_{i,j}^{n+1} + k_1 U_{i,j+1}^{n+1} + k_1 U_{i,j-1}^{n+1}$$

$$=$$

$$k_3 U_{i,j}^{n} - k_1 U_{i+1,j}^{n} - k_1 U_{i-1,j}^{n} - k_1 U_{i,j+1}^{n} - k_1 U_{i,j-1}^{n} + k_4 U_{i,j}^{n-1},$$

where we let $r = \frac{\tau}{h^2}$, and the coefficients k_1, k_2, k_3, k_4 are given in the following table.

Next, we use Von Neumann stability analysis to find a bound on the proportion of rates of change for time and space. Thus, we let $U_{i,j}^n = c_n e^{I(xi+yj)\theta}$ and directly substitute the cor-

k_1	k_2	k_3	k_4
$-r$	$(2-\alpha)+4r-2\tau f(u)$	$2(1-\alpha)-4r$	α

TABLE 3.1. Table of Coefficients

responding expressions into our finite difference scheme. After simplifying, we end up with the identity

$$(4k_1\cos(\theta)+k_2)\,c_{n+1}+(4k_1\cos(\theta)-k_3)\,c_n-k_4c_{n-1}=0.$$

Here, we assume that c_n behaves like a polynomial so that we may interpret the above relationship as a quadratic in which case we can employ the quadratic formula and find the corresponding roots to its characteristic equation:

$$R=\frac{-4k_1\cos(\theta)+k_3\pm\sqrt{(4k_1\cos(\theta)-k_3)^2-4(4k_1\cos(\theta)+k_2)(-k_4)}}{2(4k_1\cos(\theta)+k_2)}$$

Since our interest is in finding a way to avoid magnifying computational errors, we collect every term that involves the proportion of the discreet rates of change in our finite difference scheme in order to use Von Neumann stability analysis. Notice that the roots obtained from the equation above involve several terms with r. We need to check that the absolute value of these two roots is less than or equal to one. Thus we have

$$-4k_1\cos(\theta)-2k_2-k_3\leq\pm\sqrt{(4k_1\cos(\theta)-k_3)^2-4(k_1\cos(\theta)+k_2)(-k_4)}\leq 12k_1\cos(\theta)+2k_2-k_3$$

which leads us to consider two cases: the positive and negative radical. At any rate, we end up working with

$$\begin{aligned}0&\leq\sqrt{(4k_1\cos(\theta)-k_3)^2-4(k_1\cos(\theta)+k_2)(-k_4)}\\&\leq\\&\max\left\{(-4k_1\cos(\theta)-2k_2-k_3)^2,\quad(12k_1\cos(\theta)+2k_2-k_3)^2\right\}\end{aligned}$$

for both cases. Calculating the maximum on the right side of this inequality leads to

$$\max\left\{16r^2(1-\cos(\theta))^2-32r(1-\cos(\theta))-16,\quad 144r^2(1-\cos(\theta))^2+48r(1-\cos(\theta))-4\right\}$$

where we used $\alpha = \frac{1}{2}$ according to [12]. Both of the quadratic terms involved are non-negative, so we consider the situation when $16r^2(1-\cos(\theta))^2 - 32r(1-\cos(\theta)) - 16 \geq 0$ and $144r^2(1-\cos(\theta))^2 + 48r(1-\cos(\theta)) - 4 \geq 0$ so that we can find their respective roots to determine their behavior as this will specify how to chose our numerical rates of change in order to avoid amplifying computational errors. Therefore we formulate another quadratic expression where $X = r(1-\cos(\theta))$, and since both expressions are non-negative, we take their difference to simplify a bit further. For $128X^2 - 16X - 12 = 0$, we get $X = \frac{3}{8}$, and $-\frac{1}{4}$. Analyzing the behavior using a sign-chart, we see that the only bounded region is the interval $(-\frac{1}{4}, \frac{3}{8})$; i.e. if $r(1-\cos(\theta)) \in (-\frac{1}{4}, \frac{3}{8}) \leq 0$. This result is brought back into the inequality involving the maximum which is found to be the term $16r^2(1-\cos(\theta))^2 - 32r(1-\cos(\theta)) - 16$. Noting that this can be rewritten as $16\left(r(1-\cos(\theta)+1)\right)^2$, we can further examine this new quadratic in X to see that

$$X \in \left(-\frac{1}{4}, \frac{3}{8}\right)$$

$$X+1 \in \left(\frac{3}{4}, \frac{11}{8}\right)$$

$$(X+1)^2 \in \left(\frac{9}{16}, \frac{121}{64}\right)$$

$$16\,(X+1)^2 \in \left(9, \frac{121}{4}\right).$$

Hence we arrive to

$$0 \leq \sqrt{(4k_1\cos(\theta) - k_3)^2 - 4(k_1\cos(\theta) + k_2)(-k_4)} \leq \frac{121}{4}.$$

All that is left to do now is to isolate the r terms coming from the definitions of $k_1 - k_4$ while using $\alpha = \frac{1}{2}$ to end up with

$$0 < 16r^2(1-\cos\theta)^2 + 6r\cos\theta - \frac{14577}{16} \leq 0.$$

By first assuming the case when the above inequality is equal to zero, using the quadratic formula

again leads us to

$$r = \frac{-3\cos\theta \pm \sqrt{9\cos^2\theta + 14577(1-\cos\theta)^2}}{16(1-\cos\theta)^2}$$

By testing these roots with a sign chart, we find that we should choose r such that

$$0 < r = \frac{\tau}{h^2} \leq \frac{-3\cos\theta + \sqrt{9\cos^2\theta + 14577(1-\cos\theta)^2}}{16(1-\cos\theta)^2}$$

2. Another Popular Method

For the remainder of this chapter, we include some details of another well-known numerical technique whose implementation can be considered at a later time. That is to say, we do not apply this method in our current research although it would be interesting to consider extending our understanding of approximating the Allen-Cahn equation.

The Finite Element Method is a numerical technique used to solve differential equations by partitioning the domain to be approximated into a finite space and then assembling simple elements to fill in the finite space. Boundary conditions can also be imposed as we shall see. Let us see how this technique is applied by considering Poisson's equation:

$$\begin{cases} -\Delta u(x,y) = f(x,y) & \text{on } \Omega = [0,1]^2 \\ u(x,y) = 0 & \text{on } \partial\Omega. \end{cases}$$

As the problem stands, we cannot apply the Finite Element Method yet; the domain still needs to be discretized. By considering a reformulation of the problem, namely the variational form, Poisson's equation can be interpreted as a combination of the differential equation and the boundary condition as a single expression. This method relies on Green's formula which is a generalization of the integration-by-parts technique in higher dimensions:

$$v(x)u'(x) = \int_0^1 v'u'dx - \int_0^1 vu''dx$$

One should take a moment to note that we are now engaging in the area of vector calculus.

Recall that the gradient of a differentiable scalar-valued function $v : \mathbb{R}^2 \to \mathbb{R}$ is

$$\nabla v(x, y) = \left(\frac{\partial v}{\partial x}, \frac{\partial v}{\partial y} \right).$$

Now consider a differentiable vector-valued function $\mathbf{w} : \mathbb{R}^2 \to \mathbb{R}$. Applying a dot product between $\mathbf{w}$ and the Laplacian operator, we define the divergence

$$\nabla \cdot \mathbf{w} = \sum_{i=1}^{2} \frac{\partial w_i}{\partial x_i}.$$

Recalling the product rule for differentiation, we see that

$$\frac{\partial}{\partial x_i}(fg) = g\frac{\partial f}{\partial x_i} + f\frac{\partial g}{\partial x_i}.$$

Let $f = v$ and $g = \frac{\partial u}{\partial x_i}$ and then substitute these into the summation part of our divergence formula to have that

$$\sum_{i=1}^{2} \frac{\partial}{\partial x_i} \left(v\frac{\partial u}{\partial x_i} \right) = \sum_{i=1}^{2} \frac{\partial v}{\partial x_i}\frac{\partial u}{\partial x_i} + \sum_{i=1}^{2} v\frac{\partial^2 u}{\partial {x_i}^2},$$

for differentiable functions v and twice-differentiable functions u. Furthermore, we can rewrite the expression above with vector notation using the Laplacian operator and dot products:

$$\nabla \cdot (v\nabla u) = \nabla v \cdot \nabla u + v\nabla u.$$

Now we are in a position to apply our definitions to the Divergence Theorem (also known as Gauss' Theorem):

$$\int_\Omega \sum_{i=1}^{2} \frac{\partial w_i}{\partial x_i} d\Omega = \int_{\partial\Omega} \sum_{i=1}^{2} n_i w_i ds,$$

where n_i is the components of the outward-directed unit normal vector on the boundary of the domain $\partial\Omega$. Essentially, this justifies a replacement of the Laplacian operator with the normal component n_i while simultaneously switching the domain of integration from Ω to its boundary $\partial\Omega$. This result is true for functions $\mathbf{w}$ and boundaries $\partial\Omega$ that are sufficiently smooth.

Using vector notations, we can reformulate the Divergence Theorem as follows:

$$\int_\Omega \nabla \cdot \mathbf{w} d\Omega = \int_{\partial\Omega} \mathbf{n} \cdot \mathbf{w} ds,$$

where $\mathbf{n} = (n_1, n_2)$.

Our next goal is to integrate the vector-form of the product rule which will require the use of the Divergence Theorem:

$$\int_\Omega \nabla \cdot (v\nabla u) d\Omega = \int_{\partial\Omega} \mathbf{n} \cdot \nabla u ds = \int_\Omega \nabla v \cdot \nabla u d\Omega + \int_\Omega v\Delta u d\Omega.$$

By using the directional derivative, we can derive Green's formula

$$\int_{\partial\Omega} v\frac{\partial u}{\partial n} ds = \int_\Omega \nabla v \cdot \nabla u d\Omega + \int_\Omega v\Delta u d\Omega.$$

Hence, Green's formula can be interpreted as a generalization of the integration-by-parts formula to higher dimensions.

Now that we have a vector interpretation for some of the tools involved in solving Poisson's equation, we are ready to reformulate our problem as follows:

Multiply Poisson's equation by a function v, integrate over Ω, then apply Green's formula and we get that

$$\int_\Omega v f d\Omega = -\int_\Omega v\Delta u d\Omega \tag{1}$$

$$= -\int_{\partial\Omega} v\frac{\partial u}{\partial n} ds + \int_\Omega \nabla v \cdot \nabla u d\Omega = \int_\Omega \nabla v \cdot \nabla u d\Omega, \tag{2}$$

where we used the fact that v vanishes along the boundary in the last equality.

A quick note should be made here regarding the type of function that v is allowed to be. What we are seeking is a function u whose definition is independent of the differential equation. Hence, we are led to working in the function space

$$V = \{v : \int_\Omega |\nabla v|^2 d\Omega < +\infty \quad \text{and} \quad v|_{\partial\Omega} = 0\},$$

where

$$|\nabla v|^2 = \left(\frac{\partial v}{\partial x_1}\right)^2 + \left(\frac{\partial v}{\partial x_2}\right)^2.$$

This is a linear space which means that for $v, w \in V$, then $\alpha v + \beta w \in V$ for any $\alpha, \beta \in \mathbb{R}$.

Further classifications can be done by letting V be a Sobolev space so that the functions that reside in it all have bounded derivatives. A popular notation for a Sobolev space in the literature is given as $H_0^1(\Omega)$ [4].

We have now developed enough material to reformulate Poisson's Equation in the Variational Form:

$$\text{Find } u \in V \text{ such that}$$

$$\int_\Omega \nabla v \cdot \nabla u d\Omega = \int_\Omega v f d\Omega \qquad \forall v \in V.$$

A solution to this type of problem is called a weak solution. Hence, we are looking for a weak solution of Poisson's Equation by employing the Finite Element Method.

To start the process of finding a weak solution via the Finite Element Method, we first need to partition the domain Ω into non-overlapping triangles as illustrated in [4]. Each corner of a triangle are referred to as nodes: boundary nodes if they lie on the boundary of Ω and internal nodes if they are not on the boundary of Ω. We also introduce a parameter $h > 0$ to represent the accuracy of the triangulated mesh. Since we want to operate in a Sobolev space V, then let us define a subset of the entire space where we can impose our necessary conditions. Let $V_h \subset V$ be the space of all functions that are continuous on $\overline{\Omega}$, linear on each triangle, and vanishes on the boundary $\partial\Omega$. For a very detailed illustration of this setup, see [4] where we can see triangular planes.

Therefore, our original problem is modified with the finite-element discretization of the domain to become the following problem:

$$\text{Find } u_h \in V_h \text{ such that}$$

$$\int_\Omega \nabla v_h \cdot \nabla u_h d\Omega = \int_\Omega v_h f d\Omega \qquad \forall v_h \in V_h.$$

We are going to employ some algebraic tools to reach a practical interpretation of the above equation. Because of the way we defined V_h, the planar surface of u_h on each triangle is uniquely determined by the values of u_h at each triangular corner. Let N be the total number of internal nodes. We define the basis functions $\{\phi_j(\mathbf{x})\}_{j=1}^N \subset V_h$ so that every function $u_h \in V_h$ can be

expressed as

$$u_h(\mathbf{x}) = \sum_{j=1}^{N} u_j \phi_j(\mathbf{x}),$$

where u_j is the value of u_h at node j and $\phi_j(\mathbf{x})$ is the "tent" function as illustrated in [4]. Notice that ϕ_j is zero everywhere, but raises as a tent does around node j; hence, $\phi_j \in V_h$ so that

$$\phi_j(\mathbf{x}_k) = \begin{cases} 1 & \text{if} \quad k = j \\ 0 & \text{otherwise} \end{cases}$$

where $\mathbf{x}_k$ is the coordinate of node k.

Substituting our new expression for u_h into the variational form of Poisson's Equation, we see that

$$\sum_{j=1}^{N} u_j \int_\Omega \nabla v_h \cdot \nabla \phi_j d\Omega = \int_\Omega v_h f d\Omega \qquad \forall v_h \in V_h$$

Here is where the problem becomes simplified. Due to the fact that we seek solutions for all $v_h \in V_h$, then let us choose $v_h = \phi_i$ for $i = 1, \ldots, N$ so that we get a much simpler version of the above equation

$$\sum_{j=1}^{N} u_j \int_\Omega \nabla \phi_i \cdot \nabla \phi_j d\Omega = \int_\Omega \phi_i f d\Omega, \qquad i = 1, \ldots, N. \tag{3}$$

This is a system of linear equations in the coefficients u_j for $j = 1, \ldots, N$, hence we can interpret our problem as one of the form

$$\mathbf{Ax} = \mathbf{b},$$

where the matrix $\mathbf{A}$ has

$$A_{ij} = \int_\Omega \nabla \phi_i \cdot \nabla \phi_j d\Omega$$

as its components and

$$\mathbf{x} = \begin{pmatrix} x_1 \\ \vdots \\ x_n \end{pmatrix}, \qquad \mathbf{b} = \begin{pmatrix} \int_\Omega \phi_1 f \, d\Omega \\ \vdots \\ \int_\Omega \phi_N f \, d\Omega \end{pmatrix}.$$

In practice, the integration taking place on the right-hand side of the equation above is typically also approximated using Gaussian Quadrature. As a standard convention, the matrix **A** is usually called the stiffness matrix and the vector **b** is often known as the load vector [4]. Therefore, solving Poisson's Equation with the finite-element method will require that we set up and then solve a system of linear equations.

CHAPTER IV

NUMERICAL EXPERIMENTS FOR THE ALLEN-CAHN EQUATION

The Allen-Cahn equation may be classified as a reaction-diffusion equation. Generally speaking, this class of partial differential equations arises in mathematical modeling, typically, when the reactions and disbursements (diffusion) of either one or several materials are considered in a specific domain.

Let $\Omega = [-5, 5]^2 \subset \mathbb{R}^d$ be an open, rectangular and bounded region with $\epsilon = 1$ and $T > 0$. Our goal is to examine a numerical scheme for the Allen-Cahn equation with initial conditions:

$$\begin{cases} \frac{\partial u}{\partial t} = \epsilon^2 \Delta u + f(u), & x \quad \text{in} \quad \Omega \subset \mathbb{R}^d, \quad t \in [0, T], \\ u|_{t=0} = u_0, & x \quad \text{in} \quad \Omega \end{cases} \tag{4}$$

where we may impose either Dirichlet, Neumann, or periodic boundary conditions.

The function $u = u(x, y, t)$ appearing above is known as a phase-field function and assumes values between -1 and 1 around the boundary of Ω. Furthermore, the values in the region $-1 < u < 1$ are generated when mixtures occur. Also, the small parameter ϵ is the width of the interface that separates the two phases; thus it serves the crucial role of regulating the interaction between the two anti-phase domains. Since we are dealing with a reaction-diffusion equation, the nonlinear forcing term $f(u)$ in the Allen-Cahn equation is characterized as $f(u) = F'(u)$ with F being the potential energy function that is typically taken to be double-welled [1, 14, 2]. In particular, we will be using $f(u) = u^3 - u = u(u - 1)(u + 1)$ as our reaction term.

For the purposes of this thesis, we will consider the (2+1)-dimensional Allen-Cahn equation and use the classical finite difference method of Crank-Nicolson as well as a modified version according to [12] for both the time discretization and the resulting two spatial dimensional equations. Considering that we have a nonlinear forcing (reaction) term $f(u)$, we will evaluate f at the points of our mesh in order to find approximate solutions as well as impose Dirichlet boundary conditions. Furthermore, our approach is designed in a way that requires a rectangular mesh for the

spatial domain that originates from the PDE. After the discretization of the original region under investigation, we implement the five-point central difference scheme to approximate the Laplacian appearing in the Allen-Cahn equation at the specified grid points, or nodes. In order to handle the time dimension, we also consider using forward differences to end up with the Crank-Nicolson scheme as well as linear combination of forward and backward difference methods. The Crank-Nicolson method is a classical approach that combines forward and backward Euler differences and is implicit in time. That is to say, this finite difference technique requires one to solve an equation that involves both the current and subsequent stage in time in order to obtain approximate solutions. As for the development shown in [12], a linear combination of forward and backward difference methods is shown to provide reasonable numerical solutions for reaction-diffusion equations.

1. Examples and Experiments

In this section, we provide the results from our numerical schemes reported in Chapter 3 for approximating the Allen-Cahn equation. Our first numerical experiment follows closely in the steps of [15] in the sense of using a circular domain in order to observe the "shrinkage kinetics." Let $u = u(x, y, t)$ be a solution to the Allen-Cahn equation. Now let $U_{i,j}^n$ be the numerical approximation to u at time step n with location i, j. Note that we use the indices i, j to "point" at the current position in our computational grid that would correspond to the (x, y) location. In Figure **??**, we see the numerical solution using the Crank-Nicolson scheme when $\tau = 0.02, h = 0.2, \epsilon = 0.006$. The computational domain is the interval $[-5, 5]$ in both spatial dimensions and the temporal domain is $[0, 1]$. From this, we suspect that using a longer time interval will show us a smaller diffusive region. Thus, Figure **??** displays our approximation using the same scheme, but with $T = [0, 2]$ and with the subplot command so that we may see more than one image.

Additionally, we also considered the case when there are two circles inside of the computational domain, along with the Crank-Nicolson scheme, to see if that would affect any of the diffusive properties of the equation. To achieve this, the code was modified to include the geometric shapes and the sizes of their respective radii while keeping the values of $\tau, h,$ and ϵ the same as before. By choosing certain values for the size of each circle, we are able to simulate either two disjoint diffusions or an intersection between them to see how they propagate as time elapses.

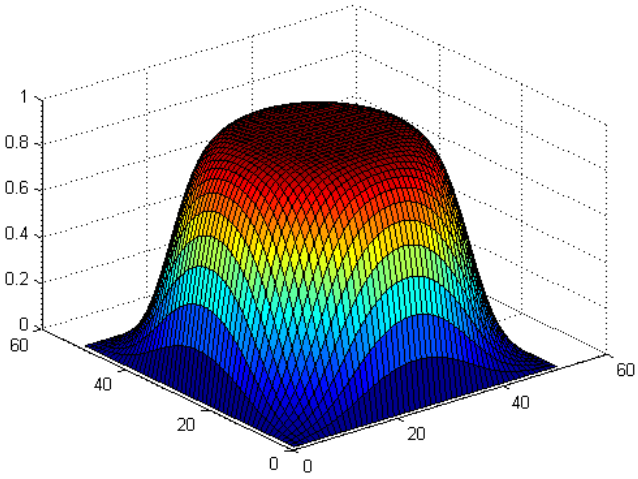

FIGURE 4.1. Crank-Nicolson Approximation 1

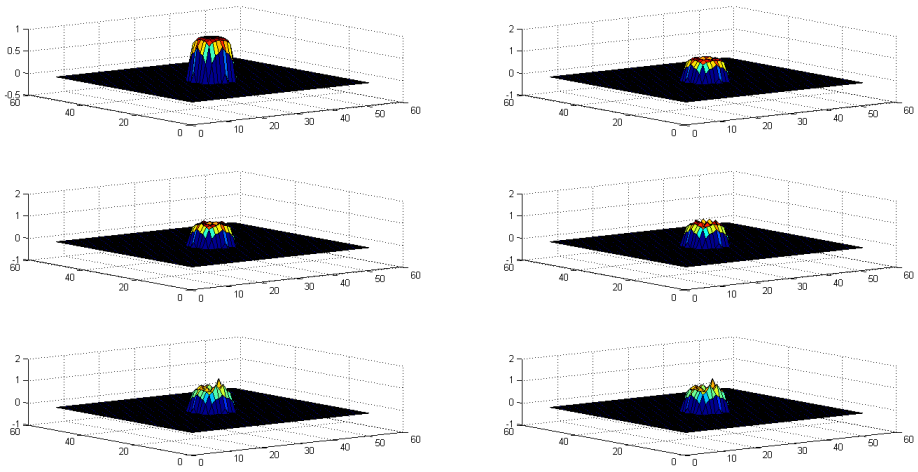

FIGURE 4.2. Crank-Nicolson Approximation 2

Figure **??** shows the first mentioned simulation from a bird's eye view and **??** displays an early stage of the latter.

Our main interest was to use the weighted approximation of the time derivative and a second-order central difference for the spatial derivatives as outlined in [12]. However, we extend the implementation of this scheme to the two-dimensional Allen-Cahn equation as opposed to the one-dimensional Fitz-Hugh Nagumo equation. Here, we refer to the number of spatial dimensions only since both of them depend on time by default. In Figure **??**, only the last outcome

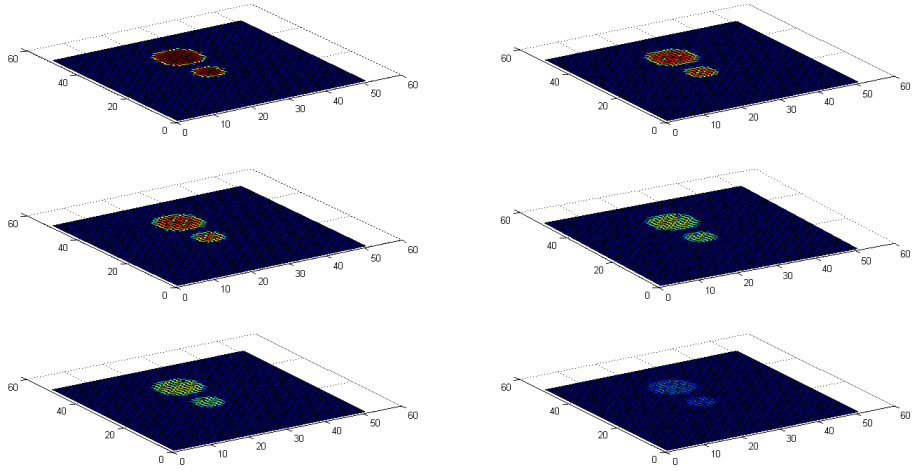

FIGURE 4.3. Two Circles

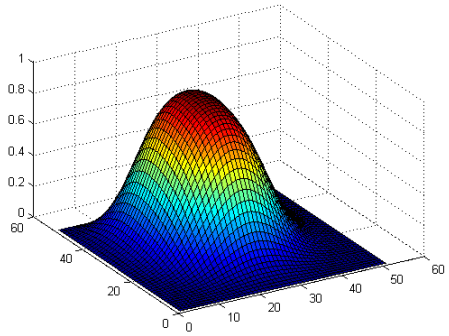

FIGURE 4.4. Diffusive Collision

is depicted when we let $\tau = 0.02$, $h = 0.2$, and $\epsilon = 0.0006$ with the time interval allowing for 100 steps and the spatial domain being uniformly-spaced among 50 points in our finite mesh.

Furthermore, we also show the results using this special finite-difference method with the same parameters as before, but with the time interval extended to $[0, 5]$ in Figure **??**. That is to say, our time interval takes 250 time steps into consideration. The subplot command is also used in order to capture the diffusive properties of our numerical solution. Figure **??** is the same weighted approximation, but with the diffusion being shown from above in order to better visualize the diffusive nature of our mathematical model. Notice how the circular region depicting our numerical solution diminishes as time goes by.

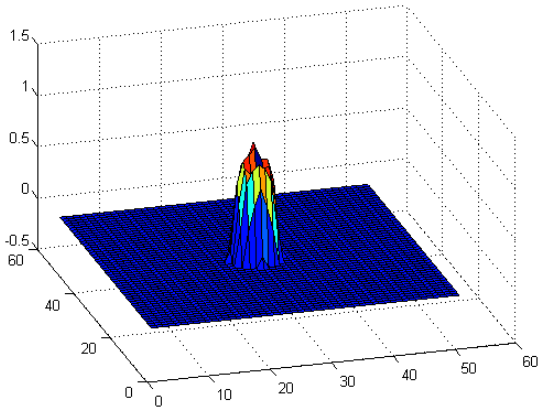

FIGURE 4.5. Modified Finite Difference Solution

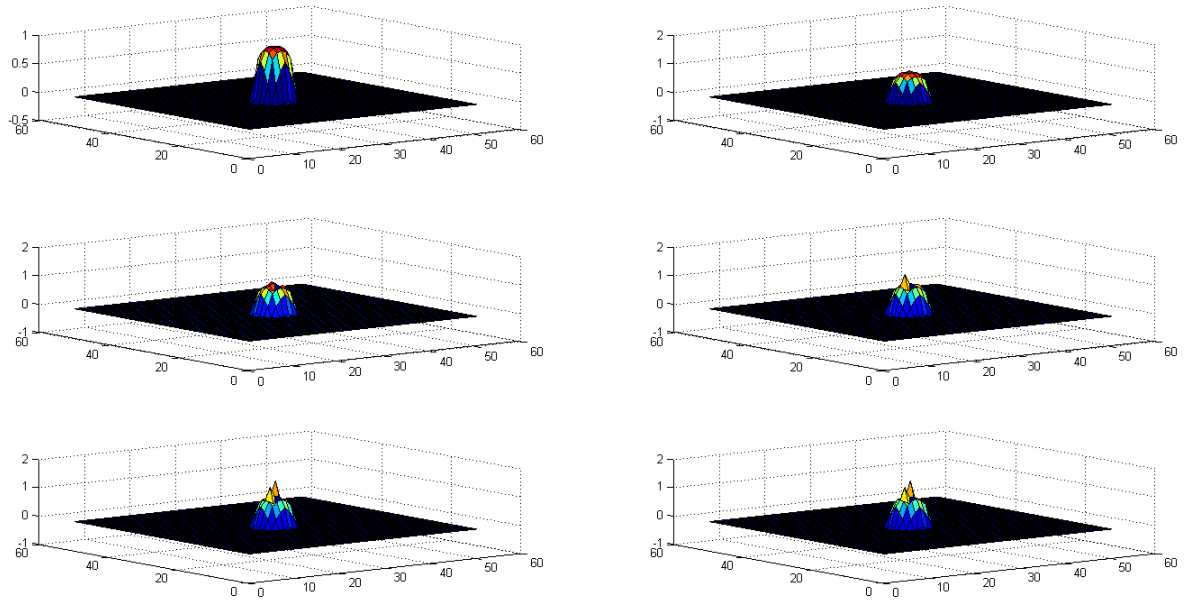

FIGURE 4.6. Weighted Approximation

Naturally, we can expect this pattern to eventually disperse completely into the computational region which is consistent with the physical background of a reaction-diffusion process. Due to physical memory limitations, the computers used to run our programs had to be restricted to using certain parameters which could, in theory, be further optimized. Nonetheless, we were still able to obtain feasible results which imply that solutions to this particular reaction-diffusion equation can be approximated using well-known numerical methods.

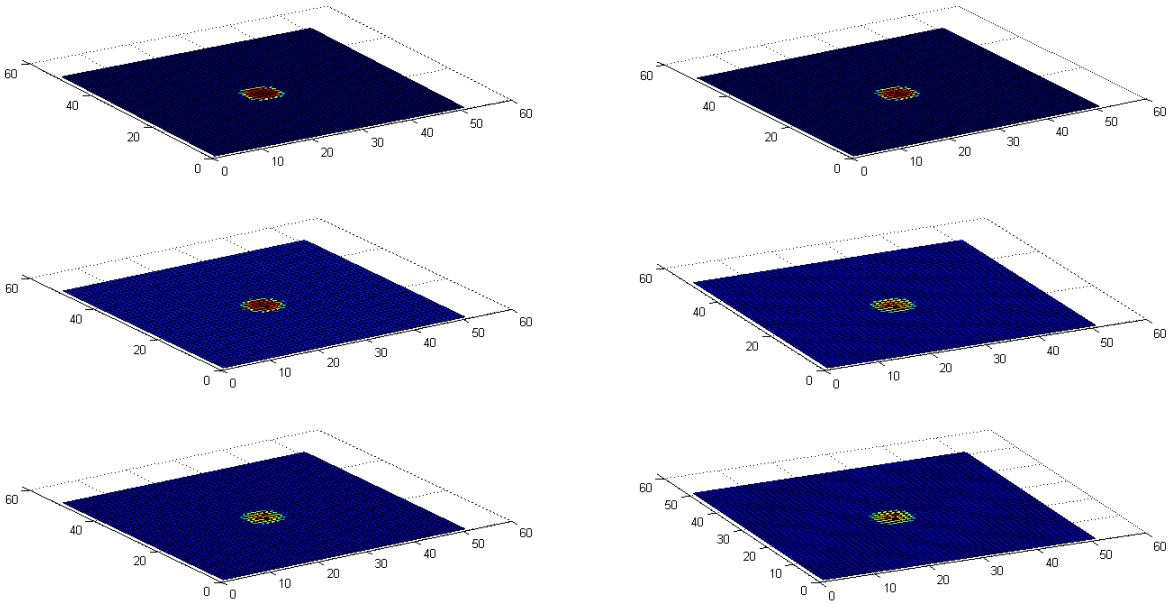

FIGURE 4.7. Overhead View of Weighted Approximation

CHAPTER V

CONCLUSION

For this thesis, we considered both the classical finite-difference method of Crank-Nicolson as well as a modified finite-difference scheme to find approximate solutions to a certain type of non-linear partial differential equation. Namely, we considered the explicit scheme outlined in [12], but in the context of the Allen-Cahn equation within a uniformly-spaced rectangular domain. However there are many more techniques available such as the finite element method as is referenced at the end of Chapter 3. For future intents and purposes, this approach can be considered when seeking to find numerical solutions to partial differential equations. Moreover, the work we have done here can be expanded and further optimized. As such, we will provide the source code used to produce our results, which was written in the script language of MATLAB, in the Appendix found at the end of this document. Nonetheless, our implementation of the explicit finite difference method found in [12] was used to find approximate solutions to the Allen-Cahn equation

$$\begin{cases} \frac{\partial u}{\partial t} = \epsilon^2 \Delta u + f(u), \quad x \quad \text{in} \quad \Omega \subset \mathbb{R}^d, \quad t \in [0, T], \\ u|_{t=0} = u_0, \qquad\qquad\quad x \quad \text{in} \quad \Omega \end{cases}$$

which led us to interesting diffusive patterns in the case when $d = 2, \quad f(u) = u^3 - u$, and using a uniformly-spaced finite mesh as our computational domain. Moreover, we extended the scope of this technique since it was originally proposed for a one-dimensional version of the Fitz-Hugh Nagumo equation. Some adjustments were also made for our numerical scheme such as using the five-point central difference to approximate the two spatial derivatives. Essentially, the approach taken in this thesis expands on the one-dimensional results of a certain weighted approximation originally carried out on a different reaction diffusion equation with one spatial derivative.

Certain parameters found in the source code reported in the Appendix were tactfully chosen according to established constants as seen in [12] and [15]. Furthermore, we also used a two-dimensional Von Neumann stability analysis technique to find suitable choices for the rates of change in time and space to ensure that the numerical errors are not magnified during the computa-

tion of our approximate solutions. To the best of our knowledge, this is the first time this weighted approximation has been applied to the (2+1)-dimensional Allen-Cahn equation. Based on the consulted literature, we sought out works that placed emphasis on numerical methods for solving partial differential equations, previous theoretical and numerical analyses of the Allen-Cahn equation and other reaction-diffusion equations, as well as a few textbooks for our definitions, history, and derivations.

REFERENCES

[1] M. Alfaro, D. Hilhorst, H. Matano. *The Singular Limit of the Allen-Cahn Equation and the FitzHugh-Nagumo System.* Journal of Differential Equations, Vol. 245, Issue 2, pp. 505-565, 2008.

[2] S. Allen and J. W. Cahn. *A Microscopic Theory for Antiphase Boundary Motion and its Application to Antiphase Domain Coarsening.* Acta Metallurgica, Vol. 27. pp. 1085-1095, Pergamon Press 1979.

[3] S. Bartels, R. Müller, and C. Ortner . *Robust A Priori and A Posteriori Error Analysis for the Approximation of Allen-Cahn and Ginzburg-Landau Equations Past Topological Changes.* SIAM Journal on Numerical Analysis, Vol. 49, No. 1, pp. 110-134, 2011.

[4] M. Berggren, *An Introduction to the Finite Element Method for Elliptic Problems*, Uppsala University, 2002.

[5] Y. Fukao, Y. Morita and H. Ninomiya, *Some Entire Solutions of the Allen-Cahn Equation,* Taiwanese Journal of Mathematics, Vol. 8, No. 1, pp. 15-32, March 2004.

[6] D. Iber, *Numerical Solution of Reaction-Diffusion Problems*, Department for Biosystems Science and Engineering (D-BSSE), ETH Zurich, Swiss Institute of Bioinformatics, Basel, Switzerland.

[7] M. Haase, *Functional Analysis, An Elementary Introduction,* American Mathematical Society, Graduate Studies in Mathematics, Vol. 156, 2014.

[8] Y. Kimura. *The Mathematics of Patterns: The Modeling and Analysis of Reaction-Diffusion Equations.* Princeton University, 2014.

[9] M. K. Kiplaga, *The Compact Implicit Integration Factor for the Solution of Allen-Cahn Equations,*(Master's Thesis), University of South Carolina Scholar Commons, 2013.

[10] R. E. Mickens, *Nonstandard Finite Difference Models of Differential Equations,* Singapore, River Edge, N.J., World Scientific, 1994.

[11] H. Ninomiya. *Traveling Wave Solutions of the Allen-Cahn Equations.* Research Institute for Mathematical Sciences Course Gives Discussions Proceedings, No. 1545, pp. 112-121, 2007.

[12] J. Ruiz-Ramirez and J. E. Macias-Diaz, *A Finite Difference Scheme to Approximate Non-*

Negative and Bounded Solutions of a Fitz-High Nagumo Equation, International Journal of Computational Mathematics, Vol. 88, No. 15, 3186-3201, October 2011.

[13] E. Tadmor, *A Review of Numerical Methods for Nonlinear Partial Differential Equations,* Bulletin (New Series) of the American Mathematical Society, Vol. 49, No. 4, pp. 507-554, October 2012.

[14] F. Zhang. *A Qualitative Research on Allen-Cahn Equations.* Ph.D. Thesis, University of Connecticut, 2011.

[15] J. Zhang and Q. Du. *Numerical Studies of Discrete Approximations to the Allen-Cahn Equation in the Sharp Interface Limit.* SIAM Journal on Scientific Computing, Vol. 31, No. 4, pp. 3042-3063, 2009.

APPENDIX

In this appendix, we report the source code that was written for each scheme mentioned in the Experiments and Examples section.

Crank-Nicolson Scheme in MATLAB

```
clear all


epsilon=0.0006;
xL=-5;xR=-xL;
yD=-5;yU=-yD;
L=xR-xL; %the length of domain
tau=0.02;    %time step "k"
h=0.2;      %spatial step
%x=(xL+h):h:(xR-h); y=(yD+h):h:(yU-h);
x=xL:h:xR; y=yD:h:yU;
r=tau/h^2;
N=L/h; T=2;
Utemp=zeros(N+1,N+1);
x0=floor((N+1)/2);y0=x0;
%%%%%%%%%%
for i=1:N+1
    for j=1:N+1
        if  ((i-x0)^2+(j-y0)^2)<=5^2
            Utemp(i,j)=1;
        end
    end
end




%%%%%%%%%
```

```
U=reshape(Utemp',(N+1)^2,1);


ab=0;


K1 = diag([0,-r*ones(1,N-1),0]);
K11 = diag([0,r*ones(1,N-1),0]);
j=0;
for t=0:tau:T

    %  for the left parts
    A = kron(diag([ones(1,N-1),0],-1),K1) + kron(diag([0,ones(1,N-1)],1),K1);
    %  for the right parts
    A1 = kron(diag([ones(1,N-1),0],-1),K11) + kron(diag([0,ones(1,N-1)],1),K11);
    for i=2:N
        Ui = Utemp(i,:);
        K2 = diag([1,(2+4*r-tau*epsilon^(-2)*(1-Ui(2:N).^2)),1]) + diag([-r*ones(1,N-1),0],
        A = A + kron(diag([zeros(1,i-1),1,zeros(1,N+1-i)]),K2);


        K22 = diag([1,(2-4*r+tau*epsilon^(-2)*(1-Ui(2:N).^2)),1]) + diag([r*ones(1,N-1),0],
        A1 = A1 + kron(diag([zeros(1,i-1),1,zeros(1,N+1-i)]),K22);


    end
     A = A+kron(diag([1,zeros(1,N-1),1]),eye(N+1));
     A1 =A1+ kron(diag([1,zeros(1,N-1),1]),eye(N+1));
     A=sparse(A); A1=sparse(A1);
     U=A\(A1*U);
     Utemp=reshape(U,N+1,N+1);
     Utemp=Utemp';
     ab=ab+1
     %mesh(Utemp)
     %pause
```

```
    if (mod(t,T/5)==0),
        j=j+1;
        subplot(3,2,j);
        surf(Utemp)
    end
end
```

Modified Finite-Difference Method Scheme in MATLAB

```
clear all

epsilon=0.0006; %0.6
xL=-5;xR=-xL;
yD=-5;yU=-yD;
L=xR-xL; %the length of domain
tau=0.02;    %time step "delta t"
h=0.2;      %spatial step
x=xL:h:xR; y=yD:h:yU;
alpha = 0.5;
r=tau/h^2;
N=L/h; T=5;
Utemp=zeros(N+1,N+1);
x0=floor((N+1)/2);y0=x0;

for i=1:N+1
    for j=1:N+1
        if  ((i-x0)^2+(j-y0)^2)<=4^2
            Utemp(i,j)=1;
        end
    end
```

```
end

U=reshape(Utemp',(N+1)^2,1);
U0=U;U1=U;

ab=0;

K1 = diag([0,-r*ones(1,N-1),0]);
K11 = diag([0,r*ones(1,N-1),0]);
j=0;
for t=0:tau:T

    %  for the left parts
    A = kron(diag([ones(1,N-1),0],-1),K1) + kron(diag([0,ones(1,N-1)],1),K1);
    %  for the right parts
    A1 = kron(diag([ones(1,N-1),0],-1),K11) + kron(diag([0,ones(1,N-1)],1),K11);
    for i=2:N
        Ui = Utemp(i,:);
        K2 = diag([1,(2*(1-alpha)+ alpha +4*r-tau*epsilon^(-2)*(1-Ui(2:N).^2)),1]) + diag(
        A = A + kron(diag([zeros(1,i-1),1,zeros(1,N+1-i)]),K2);

        K22 = diag([1,(2*(1-alpha)-4*r+tau*epsilon^(-2)*(1-Ui(2:N).^2)),1]) + diag([r*ones
        A1 = A1 + kron(diag([zeros(1,i-1),1,zeros(1,N+1-i)]),K22);

    end
     A = A+kron(diag([1,zeros(1,N-1),1]),eye(N+1));
     A1 =A1+ kron(diag([1,zeros(1,N-1),1]),eye(N+1));
     A=sparse(A); A1=sparse(A1);
     U2=A\(A1*U1+alpha*U0);
     U0=U1;U1=U2;
     Utemp=reshape(U2,N+1,N+1);
```

```
      Utemp=Utemp';
      ab=ab+1


      if (mod(t,T/5)==0),
          j=j+1;
          subplot(3,2,j);
          surf(Utemp)
      end
end
%surf(Utemp)
%subplot(2,1,1)
save SPFDM.dat Utemp -ascii
```

VITA

JAMIL MALIK VILLARREAL

- Educational Background
  - Texas A & M International University
  - Bachelor of Science
  - May 2014
  - Mathematics
  - 4006 Vidaurri Avenue, Laredo, TX, 78041
- Positions Held
  - Supplemental Instructor/Tutor
  - Graduate Research Assistant